THE JOURNAL OF BIOLOGICAL CHEMISTRY VOL. 281, NO. 36, pp. 26205–26215, September 8, 2006

Tumor Necrosis Factor-induced Long Myosin Light Chain Kinase Transcription Is Regulated by Differentiation-dependent Signaling Events

*CHARACTERIZATION OF THE HUMAN LONG MYOSIN LIGHT CHAIN KINASE PROMOTER**

Received for publication, March 7, 2006, and in revised form, May 19, 2006 Published, JBC Papers in Press, July 11, 2006, DOI 10.1074/jbc.M602164200

W. Vallen Graham[‡], Fengjun Wang[‡§], Daniel R. Clayburgh[‡1], Jason X. Cheng[‡], Bora Yoon[‡], Yingmin Wang[‡], Anning Lin[¶], and Jerrold R. Turner[‡2]

From the [‡]Department of Pathology and [¶]Ben May Institute for Cancer Research, University of Chicago, Chicago, Illinois 60637 and the [§]State Key Laboratory of Trauma, Burns and Combined Injury, Institute of Burn Research, Southwest Hospital, Third Military Medical University, Chongqing 400038, China

Myosin light chain kinase (MLCK) is expressed as long and short isoforms from unique transcriptional start sites within a single gene. Tumor necrosis factor (TNF) augments intestinal epithelial long MLCK expression, which is critical to cytoskeletal regulation. We found that TNF increases long MLCK mRNA transcription, both in human enterocytes *in vitro* and murine enterocytes *in vivo*. 5′-RACE identified two novel exons, 1A and 1B, which encode alternative long MLCK transcriptional start sites. Chromatin immunoprecipitation (ChIP) and site-directed mutagenesis identified two essential Sp1 sites upstream of the exon 1A long MLCK transcriptional start site. Analysis of deletion and truncation mutants showed that a 102-bp region including these Sp1 sites was necessary for basal transcription. A promoter construct including 4-kb upstream of exon 1A was responsive to TNF, AP-1, or NFκB, but all except NFκB responses were absent in a shorter 2-kb construct, and all responses were absent in a 1-kb construct. Electrophoretic mobility shift assays, ChIP, and site-directed mutagenesis explained these data by identifying three functional AP-1 sites between 2- and 4-kb upstream of exon 1A and two NFκB sites between 1- and 2-kb upstream of exon 1A. Analysis of differentiating epithelia showed that only well differentiated enterocytes activated the 4-kb long MLCK promoter in response to TNF, and consensus promoter reporters demonstrated that TNF-induced NFκB activation decreased during differentiation while TNF-induced AP-1 activation increased. Thus either AP-1 or NFκB can up-regulate long MLCK transcription, but the mechanisms by which TNF up-regulates intestinal epithelial long MLCK transcription from exon 1A are differentiation-dependent.

Myosin light chain kinases (MLCKs)[3] are essential regulators of actomyosin function (1). Mammalian MLCK is encoded by two separate genes; the first is expressed in skeletal and cardiac muscle whereas the second, smooth muscle MLCK, generates three different proteins, long MLCK, short MLCK, and telokin, as a result of tissue-specific transcription from separate promoters (1–6). Like all MLCKs, the 130-kDa smooth muscle, or short, MLCK includes a catalytic domain and a separate Ca^{2+}-calmodulin-dependent regulatory domain.

Long MLCK is a 210-kDa protein originally identified in cultured cells, embryonic tissues, and endothelium (2, 4, 7, 8). It contains the same catalytic and regulatory domains as short MLCK but also includes an N-terminal extension that contains six immunoglobulin-like modules and two tandem actin binding domains (9). Long MLCK must therefore be transcribed from an upstream promoter, although this promoter has not been identified.

Long MLCK is the principal form expressed in intestinal epithelial cells (8) and expression of long MLCK is increased by tumor necrosis factor (TNF) treatment of cultured intestinal epithelial monolayers (10, 11). These increases in MLCK protein expression are accompanied by increased myosin light chain phosphorylation which, in turn, leads to disruption of the epithelial barrier (12–14). This long MLCK-dependent disruption of epithelial barrier function is an important component of intestinal disease (15). For example, long MLCK knock-out mice are protected from TNF-dependent intestinal epithelial MLC phosphorylation, barrier loss, and diarrhea (16). Similar protection is conferred by pharmacological intestinal epithelial MLCK inhibition (16). While the functional significance of increased intestinal epithelial long MLCK expression has not been defined in humans, it is notable that intestinal epithelial cells of patients with inflammatory bowel disease also display increased long MLCK expression (17). This is remarkable, as inflammatory bowel disease patients are known to have epithe-

* This work was supported in part by Grants DK61931 and DK68271 from the National Institutes of Health, the Crohn's Colitis Foundation of America, The University of Chicago Digestive Disease Center (DK42086), and The University of Chicago Cancer Center (CA14599). The costs of publication of this article were defrayed in part by the payment of page charges. This article must therefore be hereby marked "*advertisement*" in accordance with 18 U.S.C. Section 1734 solely to indicate this fact.

[1] A Predoctoral Fellow of the National Institutes of Health, The University of Chicago Medical Scientist Training Program Grant (T32 GM07281).

[2] To whom correspondence should be addressed: Dept. of Pathology, The University of Chicago, 5841 South Maryland Ave., MC 1089, Chicago, IL 60637. Tel.: 773-702-2433; E-mail: jturner@bsd.uchicago.edu.

[3] The abbreviations used are: MLCK, myosin light chain kinase; AP-1, activator protein 1; ChIP, chromatin immunoprecipitation; CMF-HBSS, calcium and magnesium free-Hanks balanced salt solution; EMSA, electrophoretic mobility shift assay; IFN-γ, interferon-γ; MLC, myosin II regulatory light chain; NFκB, nuclear factor κB; RACE, rapid amplification of cDNA ends; TNF, tumor necrosis factor.

lial barrier defects that can be corrected by anti-TNF therapy (18). Thus, inducible long MLCK expression may be a critical regulator of intestinal epithelial barrier function and disease pathogenesis.

Despite data indicating the potential biological and therapeutic potential of harnessing inducible long MLCK expression, the factors that regulate this process are unknown. Using the model of TNF-induced long MLCK expression in intestinal epithelia, we now show this process to be caused by transcriptional activation. TNF increased long MLCK mRNA transcripts in cultured human intestinal epithelial cells *in vitro* and in mouse intestinal epithelial cells *in vivo*. Two novel human long MLCK transcriptional start sites, corresponding to novel exons, were identified and the promoter corresponding to one was cloned. Moreover, the sites necessary for basal and TNF-inducible transcription have been defined. Remarkably, the requirements for TNF-inducible long MLCK transcription differ in undifferentiated and well differentiated intestinal epithelial cells, suggesting that long MLCK transcription can be regulated by multiple mechanisms. These data therefore define regulation of long MLCK transcription under basal conditions as well as following cytokine stimulation and suggest that the factors responsible for long MLCK induction are dependent on cellular differentiation state.

EXPERIMENTAL PROCEDURES

Cell Culture and Cytokine Treatment—Caco-2_{BBE} cells (19) expressing the intestinal Na^+-glucose cotransporter SGLT1 (20) were maintained and cultured as monolayers as described previously (8). For studies of differentiation and cytokine responses, monolayers grown on Transwell semipermeable supports (Corning-Costar, Acton, MA) were used 3–14 days after reaching confluence, as indicated. Recombinant human IFN-γ and TNF (R&D Systems, Minneapolis, MN) were routinely added to the basal chamber without manipulating the apical media, as described previously (10). IFN-γ-priming was performed by incubation for 18 h with 10 ng/ml IFN-γ, and TNF was used at 2.5 ng/ml, both in the basal compartment (10).

Animal Model—7–10-week-old wild-type C57BL/6 female mice were injected intraperitoneally with either 5 μg of recombinant murine TNF (PeproTech Inc., Rocky Hill, NJ) in 200 μl of phosphate-buffered saline or with phosphate-buffered saline alone, as described previously (16). Animals were sacrificed 4 h after injection and jejunal epithelia isolated as previously described (16). Briefly, a section of intestine was opened lengthwise, and washed at 4 °C in Ca^{2+}- and Mg^{2+}-free HBSS (CMF-HBSS), transferred to CMF-HBSS containing 10 mM dithiothreitol and 50 nM calyculin A (Calbiochem, San Diego, CA), incubated for 30 min at 4 °C, and transferred to a fresh tube containing CMF-HBSS with 1 mM EDTA and 50 nM calyculin A. After incubation at 4 °C for 1 h, epithelial cells were dislodged by vigorous shaking, harvested by centrifugation, and placed in TRIzol (Invitrogen, Carlsbad, CA) for mRNA analysis or SDS-PAGE sample buffer for immunoblot. Animal studies were carried out in accordance with National Institutes of Health guidelines under protocols approved by the Institutional Animal Care and Use Committee at The University of Chicago.

5′ Rapid Amplification of cDNA Ends (5′-RACE)—Total RNA was isolated chromatographically from Caco-2_{BBE} cells (Qiagen, Valencia, CA), and mRNA was purified on poly-T beads (Qiagen). Antisense primer (5′-GAATCGTCCCATCTGTC-3′) positioned within exon 4 was used for first-strand cDNA synthesis. Subsequent amplification was performed using the 5′-RACE system for rapid amplification of cDNA ends (Invitrogen). In brief, cDNA was tailed with recombinant TdT and linker (dC) oligonucleotide. 5′-RACE was performed by incubating with an aliquot of first-strand cDNA, a RACE primer positioned within exon 3 (5′-CCGCTGGTGATGGGTTGC-3′), and the abridged anchor primer. PCR conditions were initial denaturation at 94 °C for 3 min, 38 cycles of 30 s at 94 °C, 1 min at 58 °C, and 1 min at 72 °C. The final extension step at 72 °C was carried out for 10 min. The resulting products were cloned into pCR2.1-TOPO (Invitrogen) and sequenced to determine the transcriptional start site(s).

In Silico Sequence Analysis—Genomic DNA sequences were downloaded from the NCBI data base. *In silico* transcription factor binding analysis was carried out using the TFSearch program with a threshold of 85. This program searches highly correlated sequence fragments versus the TFMATRIX transcription factor binding site profile data base within the TRANSFAC resources (21).

Cloning and Vector Construction—The region from −4105 to −155bp, MLCK (4 kb), and from −4105 to −10 bp, MLCK(+145), relative to the long MLCK transcriptional start site within exon 1A was amplified from human genomic DNA using forward 5′-CCGCTCGAGTGCTATTCAAACAGGAATACAA-3′ and reverse 5′-CCCAAGCTTCTCTGAACTGCAGCAGAGG-3′ or 5′-GGGTGGACTGAGGAGGAAT-3′ primers, respectively. The promoters were verified by direct sequencing and cloned into the pGL3-Basic luciferase vector (Promega, Madison, WI). The 2-kb, 1-kb, 500-bp, and 120-bp promoters were created using the same reverse primer as the 4-kb promoter, and the forward primers 5′-AAGAATGGAAATGACAGAGC-3′, 5′-CACTGTTGCATCAGGGATTA-3′, 5′-ATCCCTGATAGCCAGGAG-3′, and 5′-GTGATGTACTCCTCCCAGCC-3′, respectively. These PCR products were first cloned into pCR2.1-TOPO and subsequently sequenced and cloned into pGL3-Basic.

Deletion constructs were made by standard restriction digestion and ligation. The Δ(−2416 to −1588), Δ(−2416 to −836), Δ(−2416 to −200) constructs were made by digesting with EcoRI and ApaI, AflII and ApaI, or AleI and ApaI, respectively. Ends were blunted with T4 DNA polymerase (New England Biolabs, Ipswich, MA) and then ligated with T4 DNA ligase (New England Biolabs). The Δ(−1715 to −591), Δ(−417 to −177), and Δ(−530 to −200) constructs were made by digesting with MscI, PstI, or AleI, respectively, and then ligated with T4 DNA ligase. All final constructs were verified by sequencing.

Disruption of transcription factor binding sites was done by mutagenesis using the QuikChange site-directed mutagenesis kit (Stratagene). Sense oligonucleotides were: 5′ Sp1, 5′-GTCCCAGAGTGATGTACTACGATCAGCCGCTCCCACATCC-3′; 3′ Sp1, 5′-CTGATTTGGCTTTCCTTTACGACTTCCCACCCACCCAGG-3′; AP-1 (1), 5′-CTCCAGGGCTCTGCCCTATCAACTTAAGTACCTCCTAAA-

GGTCCTACC-3′; AP-1 (2), 5′-GACAATATGCATTTTA-CCACCAGCATAGCTAATACATAATAAACCTGGCAT-CCTCCTTCATCTC-3′; AP-1 (3), 5′-GCCCCACACCCAG-AGTTTCTTCTTAATCAAGTCTGGGGTAGGACCCAA-TAAT-3′; AP-1 (4) 5′-CTCAACCTTGAGCCTGCACCAA-GGGAACCTGGAGGACTTGTCAATACG-3′; NFκB (1) 5′-AGGACGTTTTCAGTGTGGAAGTACTATACTGAGA-TGCTGTCTTAGTCTATCTGTGC-3′; NFκB (2) 5′-CTGT-GGGACTGTAATGGGGCATGAGTTCTACCTCATCCTG-CCCC-3′. All constructs were verified by direct sequencing.

Transfection and Luciferase Assay—Promoter constructs, pNFκB-TA-Luc (Clontech, Palo Alto, CA), pAP1-Luc (Clontech, Palo Alto, CA), pJNKK2-JNK1 (23), p50–65 (24), or control pcDNA3.1 were transiently transfected in suspension into freshly trypsinized Caco-2 cells using Lipofectamine 2000 (Invitrogen). Briefly, 24 μg of DNA mixed with 60 μl of Lipofectamine 2000 in 0.5 ml of OptiMEM (Invitrogen) was added to 2×10^6 cells in a final volume of 12 ml and plated onto Transwell supports. Luciferase expression was detected using luciferin as the substrate (Promega) and measured with a Lumat LB 9507 luminometer (Berthold, Oak Ridge, TN). Preliminary studies using co-transfection with a *Renilla* luciferase expression vector showed that this transfection approach resulted in efficient and uniform transfection.

Electrophoretic Mobility Shift Assays—For protein-DNA binding reactions, 5 μg of HeLa nuclear extract protein (Promega) was incubated with ^{32}P-labeled probe or unlabeled competitors for 30 min at room temperature in a 25-μl reaction containing gel shift binding buffer (Promega). Probes were double-stranded oligonucleotides with the sense sequence AP-1 (1), 5′-CTCTTGACTTAATCACCTCCTA-3′; AP-1 (2), 5′-CCAGCAGAGCTGACACATCAGAAA-3′; AP-1 (3), 5′-CAGAGTTTCTGATTCAGCAGGTCT-3′; AP-1 (4), 5′-AGCCTGCATCAGAGTCACCTGGAG-3′; NFκB (1), 5′-GTGTGGAAGTCCCCTGCTGAAA-3′; and NFκB (2), 5′-ATGGGGTGGGAATTCCACCTCA-3′. Complexes were resolved on pre-run 4% native polyacrylamide gels and separated for 2 h at 200 V in 0.5× Tris borate/EDTA running buffer. The gels were dried, exposed to film overnight, and used for autoradiography.

Real Time RT-PCR—Cell extracts in TRIzol were sonicated, and RNA was extracted with chloroform, precipitated with isopropyl alcohol, and resuspended in diethyl pyrocarbonate-treated water. RNA was further purified using a RNeasy mini kit (Qiagen). cDNA was generated from 2 μg of RNA using Thermoscript reverse transcriptase (Invitrogen) and random hexamer primers in a 25-μl reaction. Long MLCK mRNA expression was determined by SYBR green real-time PCR through 50 cycles using the MyiQ Real-Time PCR Detection System (Bio-Rad). GAPDH was used as a reference. Primers were 5′-CAC-CGTCCATGAAAAGAAGAGTAG-3′ and 5′-GAGAGGCC-CTGCAGGAAGATGG-3′ for detection of human long MLCK, 5′-GCGTGATCAGCCTGTTCTTTCTAA-3′ and 5′-GCCCCATCTGCCCTTCTTTGACC-3′ for detection of murine long MLCK, and 5′-CTTCACCACCATGGAGAA-GGC-3′ and 5′-GGCATGGACTGTGGTCATGAG-3′ for detection of human and murine GAPDH.

SDS-PAGE and Immunoblot Analysis—Cell lysates were separated by SDS-PAGE and transferred to polyvinylidene difluoride membranes, as described previously (10, 16). MLCK was detected using the K36 monoclonal antibody (Sigma). After incubation with peroxidase-conjugated secondary antibodies (Cell Signaling Technology, Danvers, MA), blots were visualized by enhanced chemiluminescence as described previously. Densitometry of immunoblot data were performed using Metamorph 6.2 (Universal Imaging Corp., Downingtown, PA).

Chromatin Immunoprecipitation—Chromatin immunoprecipitation assays were performed using the EZChIP kit (Upstate Group, Charlottesville, VA). Caco-2 cells grown to differentiation were fixed in 1% formaldehyde at room temperature for 10 min. 125 mM glycine was added for 5 min to quench unreacted aldehydes. Cells were washed twice with ice-cold phosphate-buffered saline containing protease inhibitors (Protease Inhibitor Mixture II, Upstate Group), scraped, and collected by centrifugation at 4 °C. Cells were resuspended in SDS lysis buffer containing protease inhibitors, incubated for 10 min on ice, and sonicated four times for 10 s at 8 watts to shear DNA. After sonication, the lysate was centrifuged at 13,000 rpm for 10 min at 4 °C. The supernatant was diluted in ChIP dilution buffer (0.01% SDS, 1% Triton X-100, 1.2 mM EDTA, 16.7 mM Tris-HCl, pH 8.1, 167 mM NaCl, and protease inhibitors). Immunoprecipitation used antibodies to Sp1 (Upstate Group), Jun (Cell Signaling Technology), and NFκB (Invitrogen) added to the supernatant and incubated overnight at 4 °C with rotation. Immune complexes were collected on protein G-agarose in a solution containing 0.4 μg/μl sonicated salmon sperm DNA and washed sequentially with low salt wash buffer (0.1% SDS, 1% Triton X-100, 2 mM EDTA, 20 mM Tris-HCl, pH 8.1, and 150 mM NaCl), high salt wash buffer (0.1% SDS, 1% Triton X-100, 2 mM EDTA, 20 mM Tris-HCl, pH 8.1, and 500 mM NaCl), LiCl wash buffer (0.25 M LiCl, 1% IGEPAL-CA630, 1% deoxycholic acid, 1 mM EDTA, and 10 mM Tris-HCl, pH 8.1), and finally Tris/EDTA buffer (10 mM Tris-HCl and 1 mM EDTA, pH 8.0). Immune complexes were eluted with elution buffer (1% SDS, 0.1 M $NaHCO_3$, and 200 mM NaCl) and cross-linking was reversed by heating at 65 °C overnight. RNA was degraded with RNase A for 30 min, and protein was degraded with Proteinase K for 2 h. DNA was purified using the EZChIP polypropylene spin column and subjected to PCR amplification using the primers specific for the detection of the Sp1 (forward, 5′-CCGTCATGGTTCTGCGTCTGT-3′ and reverse, 5′-AAGGAGGAAAGGAAAGCCAAATCA-3′), AP-1 (1) (forward 5′-AAAAAGGGCCTCACCAGTTCG-3′ and reverse 5′-GCCCTCCATAAGCTACCCATCCA-3′), AP-1 (2) (forward 5′-TTCTAACAAGTTCCCAGGTGATGC-3′ and reverse 5′-AGAGATGAAGGAGGATGCCAGGTT-3′), AP-1-(3/4) (forward 5′-GTTTCTCAAAGTGTGGTCCCTAATT-AGC-3′ and reverse 5′-CCCTCCGTCTCTGAGCCTAATAGA-3′), and NFκB(1/2) (forward 5′-CTGCTGACACTTCCTGT-CCA-3′ and reverse 5′-AGAGGGTGGAAACCCTGAGT-3′) sites.

RESULTS

TNF Up-regulates Long MLCK Transcription and Protein Expression in Vitro and in Vivo—TNF treatment of IFN-γ-primed Caco-2 intestinal epithelial cell monolayers causes bar-

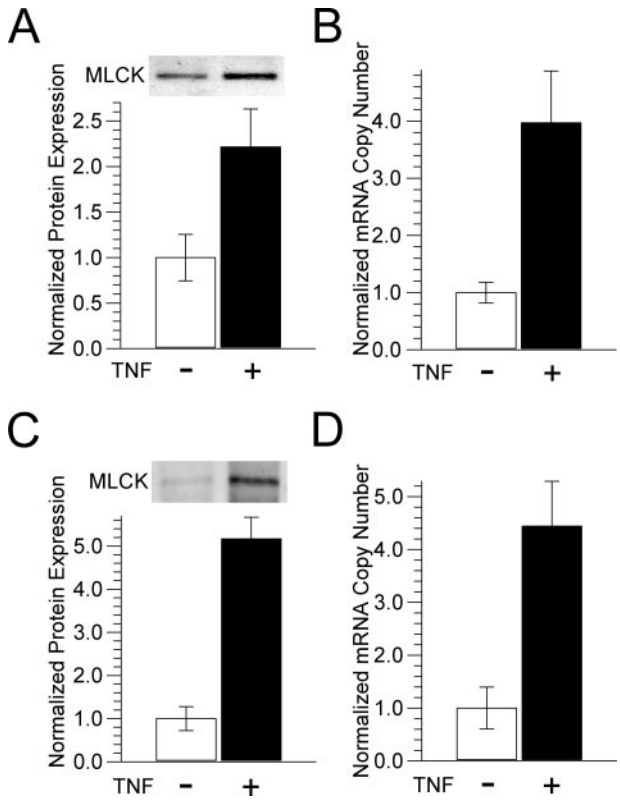

FIGURE 1. **MLCK protein and mRNA are increased after TNF treatment both *in vitro* and *in vivo*.** *A,* Caco-2 monolayers primed by 18h of culture in basal media with 10 ng/ml IFN-γ were transferred to fresh basal media with or without 2.5 ng/ml TNF, as indicated, and harvested after 4 h. Lysates were separated by SDS-PAGE and analyzed by immunoblot. TNF treatment induces marked increases in long MLCK protein expression. Quantitative data shown are mean ± S.E. of triplicate samples and are representative of more than 10 similar experiments. *B,* IFN-γ-primed monolayers were harvested 4 h after transfer to media with TNF, as above. Quantitative real time RT-PCR shows that long MLCK mRNA is increased by TNF treatment. Data shown are mean ± S.E. of duplicate samples and are representative of three similar experiments. *C,* mice were injected intraperitoneally with 5 μg of recombinant murine TNF. 4 h after injection, mice were sacrificed and jejunal epithelial cells isolated. Cell lysates were separated by SDS-PAGE and analyzed by immunoblot. TNF treatment induces marked increases in long MLCK protein expression. Quantitative data shown are mean ± S.E. of duplicate samples and are representative of five similar experiments. *D,* Jejunal epithelial cells were harvested 4 h after intraperitoneal TNF injection, as above. Quantitative real time RT-PCR shows that long MLCK mRNA is increased by TNF treatment. Data shown are mean ± S.E. of duplicate samples and are representative of three similar experiments.

rier dysfunction via increased myosin II regulatory light chain (MLC) phosphorylation (10, 12). We and others (10, 11) have recently shown that these increases in MLC phosphorylation are accompanied by increased long MLC kinase (MLCK) protein expression. Typically, a 1–2-fold increase in MLCK protein, as detected by SDS-PAGE immunoblot, is induced by TNF (Fig. 1*A*; $p < 0.02$). Quantitative real time RT-PCR analysis shows that this is accompanied by 3.0 ± 0.4-fold increase in long MLCK transcription (Fig. 1*B*; $p < 0.05$).

To determine whether these TNF-induced increases in MLCK transcription and expression also occur *in vivo*, mice were injected intraperitoneally with recombinant murine TNF. Jejunal epithelial cells were isolated 4 h after TNF injection and analyzed by SDS-PAGE immunoblot and quantitative real time RT-PCR. MLCK protein content of jejunal epithelial cells increased 4.2 ± 0.5-fold over this period (Fig. 1*C*, $p < 0.01$) and MLCK mRNA transcript number increased 3.4 ± 0.8-fold over the same period (Fig. 1*D*; $p < 0.01$). Thus, TNF activates long MLCK transcription both *in vivo* and *in vitro*. Given that increased MLCK expression is associated with barrier dysfunction (10) and has been observed in patients with inflammatory bowel disease (17), we sought to identify the regulatory elements that control long MLCK expression.

Identification of Multiple Long MLCK 5′-Untranslated Regions and Alternative Transcriptional Start Sites—The data above show that long MLCK expression is transcriptionally up-regulated by TNF. We therefore aimed to define the long MLCK promoter. Although the position of the MLCK transcriptional start site has been proposed based on models of gene structure (22), newly identified cDNA sequences (*e.g.* BC064695) that extend beyond the proposed transcriptional start site have raised uncertainty regarding the accuracy of this identification. We therefore performed 5′-RACE on mRNA isolated from Caco-2 cells using a long MLCK 3′-PCR primer within the coding region of exon 3. Two reaction products were identified and sequenced (DQ642691 and DQ642692). BLAST searches against the human genome localized both of these sequences to the long MLCK (MYLK) gene on chromosome 3q21. Neither has been previously reported among human cDNA sequences. Therefore, these sequences each represent a new transcriptional start site and corresponding first exons, exon 1A and 1B, for long MLCK (Fig. 2*A*). Notably, the translational start site and coding sequences, located within exon 2, were identical for the two transcripts. The portion of exon 3 within each sequence was also identical. Thus exons 1A and 1B represent alternative transcriptional start sites for long MLCK in Caco-2 intestinal epithelial cells.

In Silico Analysis of Putative Long MLCK Promoters—The data above show that long MLCK expression is transcriptionally up-regulated by TNF in both human-derived Caco-2 intestinal epithelial cells and murine intestinal epithelial cells. We took advantage of this to preliminarily characterize sequence upstream of the two 5′-untranslated regions we identified for long MLCK expressed in Caco-2 intestinal epithelial cells. Because TNF-induced transcriptional activation is largely mediated by AP-1 and NFκB (25), we compared potential binding sites for these transcription factors in sequences upstream of human exons 1A and 1B and the predicted mouse transcriptional start site (Fig. 2*B*). All three sequences contained numerous AP-1 and NFκB sites, but only the sequence upstream of exon 1A contained NFκB sites within 2 kb of the transcriptional start site. Given that both NFκB-dependent and -independent long MLCK up-regulation has been reported after TNF treatment of Caco-2 intestinal epithelial cells (10, 11), we therefore focused on the sequence upstream of exon 1A. We restricted our analysis to 4 kb, because all predicted AP-1 and NFκB sites were within that region (Fig. 2*B*).

Identification of Elements Necessary for Transcription from the Human Long MLCK Promoter—The sequence upstream of exon 1A was cloned into a luciferase reporter vector and included four putative AP-1 sites 1115-, 3433-, 3713-, and 3771-bp upstream of the transcriptional start site and two putative NFκB sites 1415-bp and 1584-bp upstream of the transcrip-

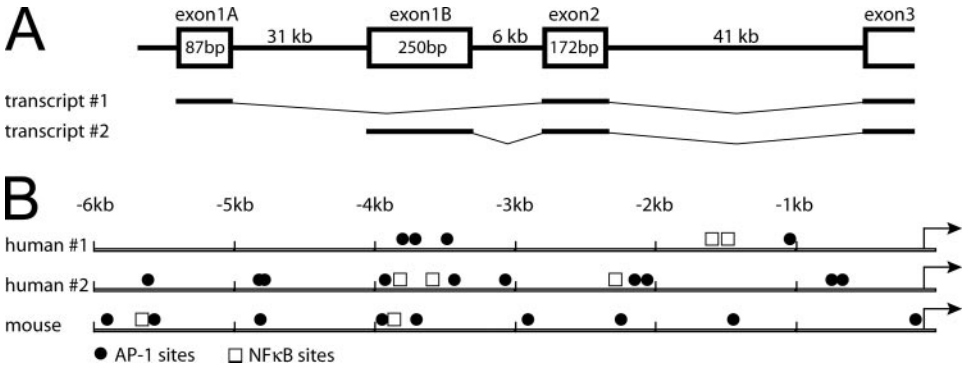

FIGURE 2. **Characterization of the MLCK transcriptional start sites.** *A*, 5′-RACE analysis reveals two alternative transcriptional start sites in Caco-2 cells. Transcript 1 utilizes the transcriptional start site encoded by the 87-bp exon 1A resulting in a 91-bp 5′-untranslated region. Transcript 2 utilizes the transcriptional start site excoded by the 250-bp exon 1B resulting in a 254-bp 5′-untranslated region. *B*, *in silico* analysis of the sequence upstream from the long MLCK transcriptional start sites. 6 kb of sequence upstream of both human transcriptional start sites and the predicted murine long MLCK transcriptional start site was analyzed for potential AP-1 (*closed circles*) and NFκB (*open boxes*) binding sites. AP-1 and NFκB sites are present in both sequences over the first 4 kb of sequence upstream of the transcriptional start sites.

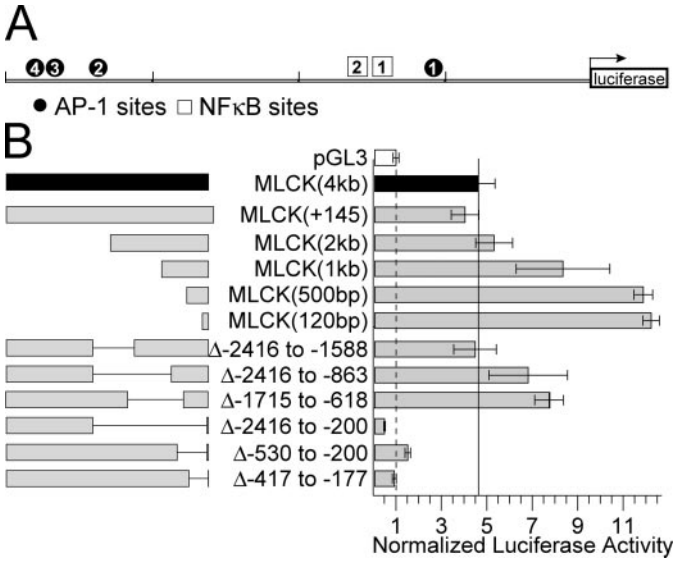

FIGURE 3. **Regions required for unstimulated human long MLCK transcription.** *A*, map showing the location of 4 potential AP-1 sites and 2 potential NFκB sites within the cloned 4-kb long MLCK promoter for the exon 1A transcriptional start site (Fig. 2*A*). *B*, luciferase expression from a series of 4-kb long MLCK constructs shows that the region from −278 to −177 bp relative to the transcriptional start site contains the minimal elements necessary for transcriptional activity. Data shown are mean ± S.E. of triplicate samples, normalized to pGL3 (*dashed line*). The activity of the 4-kb promoter is indicated for reference (*solid line*). Data are representative of three independent experiments.

tional start site (Fig. 3*A*). To assess the potential requirement for other regulatory sequences in unstimulated long MLCK transcription, a series of truncated promoter constructs was analyzed (Fig. 3*B*). Transcription from the 4-kb construct, the MLCK(+145) construct with a 145 bp 3′ extension, and a 2-kb construct were all similar. In contrast, both 500- and 120-bp constructs demonstrated transcriptional activity more than twice as great as the 4-kb construct (Fig. 3*B*). The 1-kb construct supported transcription at a level intermediate between 2- and 500-bp constructs. These data show that the 120-bp construct contains all of the elements necessary for unstimulated long MLCK transcription and further suggests that the region between 500 bp and 2 kb suppresses transcription.

To further define the sites of this suppressor activity, a series of deletion mutants were analyzed. The suppressor activity was present in a 4-kb promoter with the −2416- to −1588-bp region deleted, but was partly lost when this deletion was extended to −863 bp. The activity of a Δ(−1715 to −618)-bp construct was similar to the Δ(−2416 to −863)-bp construct. Together with the intermediate activity of the 1-kb promoter, these data suggest that sites between −1588 and −433 bp contribute to the observed suppressor activity.

Further analysis of deletion mutants lacking varying lengths of sequence between −2416 and −177 bp demonstrate that these sequences are necessary for unstimulated long MLCK transcription. Thus, together with the 120-bp construct, which extends from −278 to −155 bp, these data show that the region from −278 to −177 bp relative to the transcriptional start site is essential for long MLCK transcription.

Human Long MLCK Transcription Requires Two Sp1 Sites—To evaluate the role of the −278 to −177-bp region, this sequence was evaluated *in silico* (Fig. 4*A*). Although no TATA box was identified, two putative Sp1 sites were present 275- and 218-bp upstream of the transcriptional start site. Site-directed mutagenesis of either site-reduced transcription to only 6.0% ± 0.4% and 7.6% ± 0.5% of the wild-type 4-kb construct, a level similar to that of the promoterless pGL3 vector (Fig. 4*B*). To determine if Sp1 binds to this DNA region *in vivo*, ChIP analysis was used. Sp1 was immunoprecipitated from Caco-2 cell nuclear extracts and the associated DNA assessed by PCR amplification. The DNA sequence including the two Sp1 sites, −433 to −201 bp, was specifically immunoprecipitated with anti-Sp1, but not control, antisera (Fig. 4*C*). This suggests that these sequences are *bona fide* Sp1 binding sites. Together with the mutagenesis data, these results show that DNA sequence 5′ to the long MLCK transcriptional start site binds to Sp1 and that these Sp1 sites are required for long MLCK transcription.

The 4-kb MLCK Promoter Is Responsive to TNF—Although the data above suggest that only the first 278-bp upstream of the transcriptional start site are required for long MLCK transcription, the preliminary *in silico* analyses suggested that relevant regulatory sites may be present as much as 4-kb upstream (Fig. 3*A*). These include NFκB and AP-1 sites that might be activated by TNF. To determine the functional domains necessary for TNF-dependent MLCK transcriptional up-regulation, we first asked whether the 4-kb putative MLCK promoter was sufficient to confer TNF responsiveness. TNF alone induced a modest 0.6 ± 0.05-fold increase in transcription (Fig. 5). This is consistent with our previous demonstration that TNF alone caused only small statistically insignificant increases in MLCK protein expression (10). IFN-γ alone also failed to activate transcription from the 4-kb long MLCK pro-

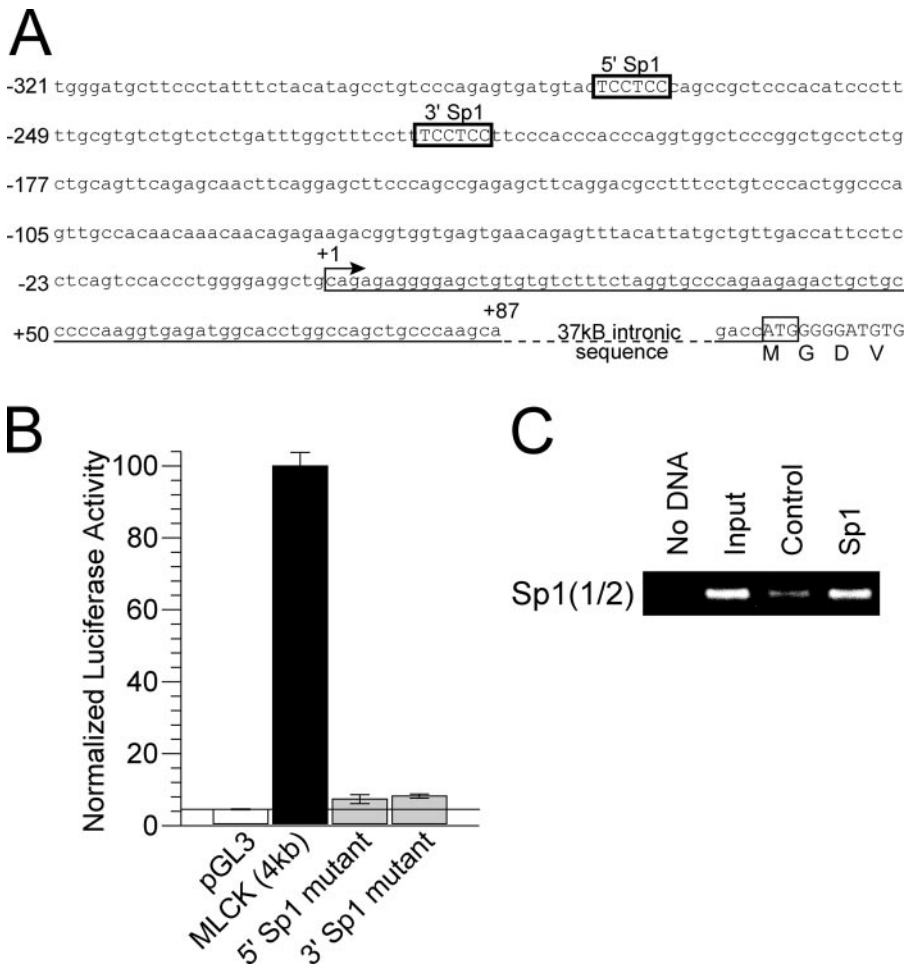

FIGURE 4. **Identification of Sp1 sites within the 4-kb long MLCK promoter.** *A*, sequence analysis of the 321-bp upstream of the translational start site identifies two putative Sp1 sites but no TATA box. The indicated intronic sequence includes exon 1B, which is not used in this transcript. *B*, although the 4-kb long MLCK promoter was sufficient to drive expression of luciferase from a reporter construct, site-directed mutagenesis of either Sp1 site reduced transcription to levels similar to a promoterless control vector (pGL3). Data shown are mean ± S.E. of quadruplicate samples, normalized to the 4-kb long MLCK construct, and are representative of two similar experiments. *C*, chromatin from Caco-2 monolayers was immunoprecipitated using antibodies against Sp1 protein. PCR analysis using primers surrounding the Sp1 sites shows that this DNA sequence (−433 to −201 bp) is specifically immunoprecipitated, indicating that Sp1 binds to sites within this sequence.

moter (Fig. 5). However, when monolayers were treated with IFN-γ and TNF, transcription increased by 1.8 ± 0.2-fold (Fig. 5). The data indicate that the 4-kb MLCK promoter is responsive to cytokine treatment in a manner that parallels endogenous MLCK expression. This suggests that the 4-kb sequence cloned contains the functional elements necessary for regulated MLCK expression.

The 4-kb MLCK Promoter Is Activated by AP-1 and NFκB—Major transcription factor signaling pathways used by TNF to induce gene expression include AP-1 and NFκB (25). To determine if either of these transcription factors is able to activate transcription from the 4-kb MLCK promoter, cells were co-transfected with the promoter construct and vectors that increase AP-1- or NFκB-dependent transcription. AP-1-dependent transcription was activated using a constitutively active JNKK2-JNK1 fusion construct (23). This increased luciferase expression from an AP-1 consensus promoter by 2.6 ± 0.3-fold (Fig. 6*A*, $p < 0.01$). The JNKK2-JNK1 fusion construct has no significant activating effect on expression from a promoterless luciferase construct or from a luciferase reporter vector with a consensus NFκB promoter (Fig. 6*A*). When MLCK promoters were analyzed, the JNKK2-JNK1 fusion construct did not augment expression from either a 1- or a 2-kb MLCK promoter (Fig. 6*B*), but did increase expression from the 4-kb MLCK promoter reporter by 1.5 ± 0.1-fold (Fig. 6*B*; $p < 0.01$). Thus, the 4-kb MLCK promoter is responsive to AP-1 and critical regulatory sequences are present between 2- and 4-kb upstream of the transcriptional start site.

NFκB-dependent MLCK transcription was analyzed similarly using an NFκB p50–65 fusion protein construct (24). Transfection of Caco-2 cells with this p50–65 construct increased luciferase expression from an NFκB consensus promoter by 2.5 ± 0.2-fold (Fig. 7*A*, $p < 0.01$). The p50–65 fusion construct had no effect on expression from a promoterless luciferase construct, but markedly suppressed expression from a luciferase reporter vector with a consensus AP-1 promoter (Fig. 7*A*, $p < 0.01$), consistent with the emerging model of NFκB-AP-1 suppressive cross-talk (26). When MLCK promoters were analyzed, the p50–65 fusion construct did not augment expression from a 1-kb MLCK promoter, but did increase transcription from the 2- and 4-kb MLCK promoters by 4.1 ± 0.1-fold and 2.0 ± 0.2-fold, respectively (Fig. 7*B*; $p < 0.01$). Thus, the 4-kb MLCK promoter is responsive to NFκB. Moreover, these data indicate that the critical regulatory sequences necessary for the NFκB response are present between 1- and 2-kb upstream of the transcriptional start site.

Characterization of AP-1 and NFκB Binding Sites within the 4-kb MLCK Promoter—The data above show that both AP-1 and NFκB are able to increase transcription from the 4-kb MLCK promoter. Together with the *in silico* analyses showing that the 4-kb sequence contains four potential AP-1 sites and two potential NFκB sites (Fig. 3*A*), these data suggest that one or more of these sites may be involved in MLCK transcriptional regulation. To assess the functionality of these potential transcription factor binding sites, we first used electrophoretic mobility shift assay (EMSA) to determine if the sites were able to bind nuclear protein. Nuclear extracts caused a probe containing the AP-1 (1) site at −1115 to shift (Fig. 8*A*). This shift was specifically and efficiently competed by unlabeled AP-1 (1) oligonucleotide or an AP-1 consensus oligonucleotide. Simi-

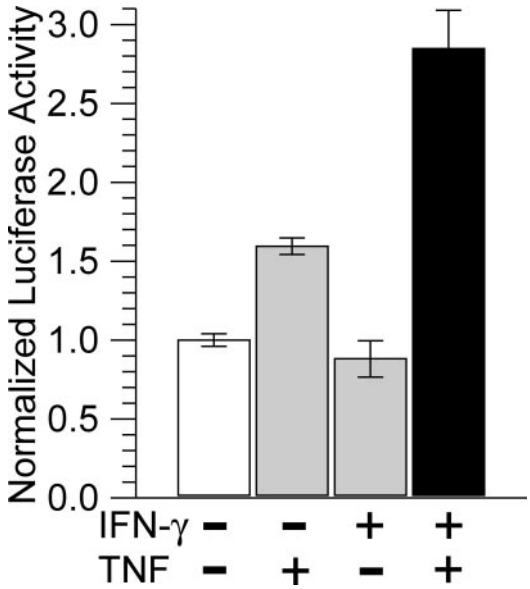

FIGURE 5. **The human long MLCK promoter is activated by IFN-γ and TNF.** Caco-2 cells transiently transfected with the 4-kb promoter construct were plated on Transwell inserts. At 14 days postconfluence the monolayers were treated with TNF alone, IFN-γ alone, or IFN-γ and TNF together, as indicated. Whereas modest increases in promoter activity were induced by TNF alone, the greatest induction resulted from combined treatment with IFN-γ and TNF. Data shown are mean ± S.E. of triplicate samples, normalized to control without cytokines, and are representative of four similar experiments.

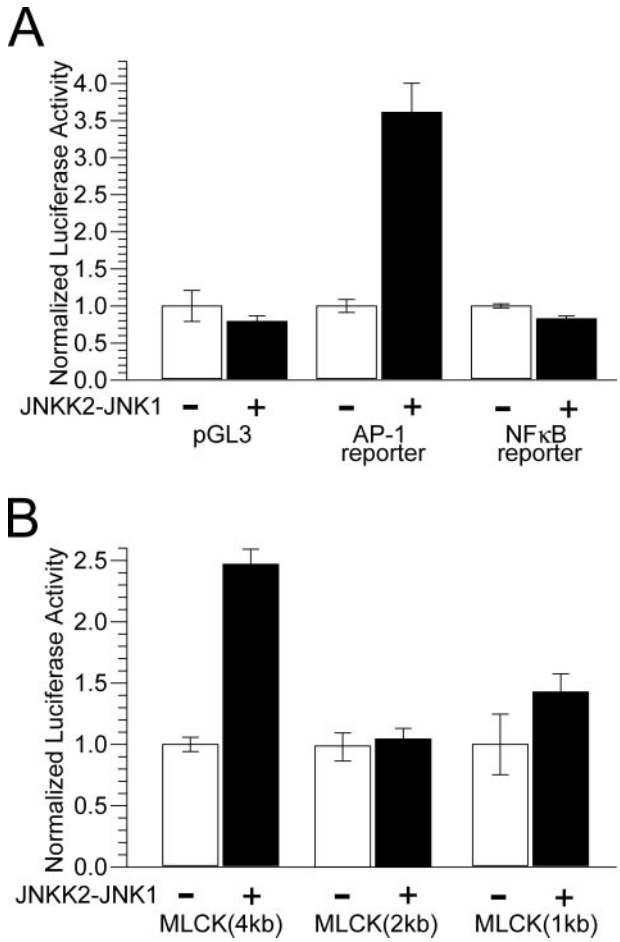

FIGURE 6. **AP-1 is sufficient to up-regulate transcription from the long MLCK promoter.** *A,* Caco-2 cells were cotransfected with promoter-reporter constructs and a JNKK2-JNK1 expression construct that activates endogenous AP-1, as indicated. The data show significant activation of only the AP-1 reporter construct. These results confirm that AP-1 signaling is activated and NFκB signaling is not activated by the JNKK2-JNK1 fusion protein. Data shown are mean ± S.E. of triplicate samples, normalized to transfection with the reporter construct and an empty vector, and are representative of three similar experiments. *B,* cotransfection of Caco-2 cells with the JNKK2-JNK1 expression construct and the 4-kb long MLCK promoter reveals significant activation for the 4-kb promoter. In contrast, 2- and 1-kb promoters respond with only a small nonsignificant increase in luciferase expression. Data shown are mean ± S.E. of triplicate samples, normalized to control transfection with the reporter construct and an empty vector, and are representative of four similar experiments.

larly, probes including the AP-1 (2), AP-1 (3), and AP-1 (4) sites, at −3433, −3713, and −3771 bp, respectively, were shifted in EMSA analysis and these shifts could be competed with both site-specific and AP-1 consensus oligonucleotides. These data suggest each of these putative AP-1 binding sites binds to AP-1 *in vitro*.

To determine if AP-1 is associated with these sites in Caco-2 cells, nuclear extracts were assessed by ChIP. The AP-1 (1), AP-1 (2), and AP-1(3/4) sites were not detected in AP-1 immunoprecipitates from control Caco-2 cells (Fig. 7*B*). As AP-1 (3) and AP-1 (4) sites are only separated by 58 base pairs, they cannot be resolved by PCR in ChIP assays. When nuclear extracts from IFN-γ-primed TNF-treated Caco-2 cells were analyzed, AP-1 immunoprecipitates contained more AP-1 (1), AP-1 (2), and AP-1(3/4) site DNA, relative to control cells (Fig. 7*B*). As AP-1 (2) and AP-1 (3) sites are only separated by 280 base pairs, the ChIP data should be interpreted to indicate that AP-1 (1) as well as at least one of the AP-1 (2), AP-1 (3), and AP-1 (4) sites bind to AP-1 in a TNF-inducible fashion.

EMSA analysis of the two putative NFκB sites, −1415 and −1584 bp, identified within the MLCK promoter also demonstrated shifts when co-incubated with nuclear extracts (Fig. 8*C*). These bands could be specifically and efficiently competed using either site-specific cold oligonucleotides or NFκB consensus oligonucleotides, suggesting that NFκB binds to each of these sites *in vitro*. To assess the ability of NFκB to interact with sites in Caco-2 cells, ChIP analysis was performed using NFκB immunoprecipitates, but NFκB(1/2) DNA was not recovered (Fig. 8*D*). This suggests that TNF does not induce NFκB binding to these sites within the MLCK promoter in Caco-2 cells.

Site-directed Mutagenesis of Specific Transcription Factor Binding Sites Ablates Transcriptional Activation—Together with the responsiveness of the 4-kb promoter to AP-1 and NFκB activation by JNKK2-JNK1 and p50–65 fusion proteins, respectively, the EMSA and ChIP data suggest that the transcription factor binding sites identified may be involved in regulation of MLCK transcription. To determine the specific roles of these sites in MLCK transcriptional regulation each site was disrupted by site-directed mutagenesis. Disruption of the AP-1 (1) site resulted in only mild reduction of luciferase expression (Fig. 9*A*). In contrast, mutagenesis of AP-1 (2), AP-1 (3), or AP-1 (4) sites markedly reduced the ability of JNKK2-JNK1 fusion protein to increase transcription (Fig. 9*A*). These data indicate that AP-1 sites 2, 3, and 4 are each required for transcriptional regulation of MLCK by AP-1. In contrast, the AP-1 (1) site appears to be at least partially dispensable.

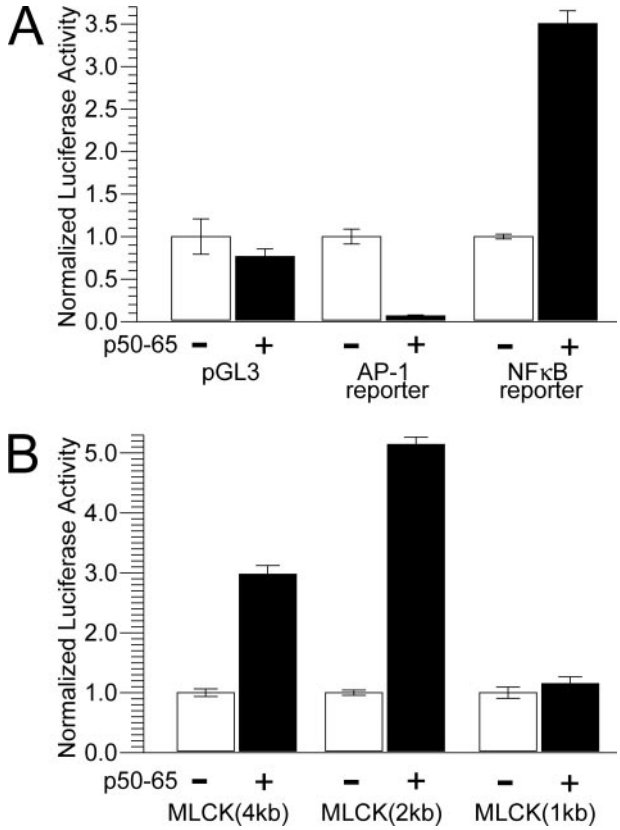

FIGURE 7. **NFκB is sufficient to up-regulate transcription from the long MLCK promoter.** *A,* Caco-2 cells were cotransfected with promoter-reporter constructs and a p50–65 expression construct that expresses a constitutively-active NFκB fusion protein. The data show significant activation of the NFκB reporter construct and significant repression of the AP-1 reporter construct. These results confirm that NFκB signaling is activated, and AP-1 signaling is not activated by the p50–65 fusion protein. Data shown are mean ± S.E. of triplicate samples, normalized to transfection with the reporter construct and an empty vector, and are representative of three similar experiments. *B,* cotransfection of Caco-2 cells with the p50–65 expression construct and the 4-kb long MLCK promoter reveals significant activation for 4- and 2-kb promoters. In contrast, no increase in expression is induced from the 1-kb promoter. Data shown are mean ± S.E. of triplicate samples, normalized to control transfection with the reporter construct and an empty vector, and are representative of four similar experiments.

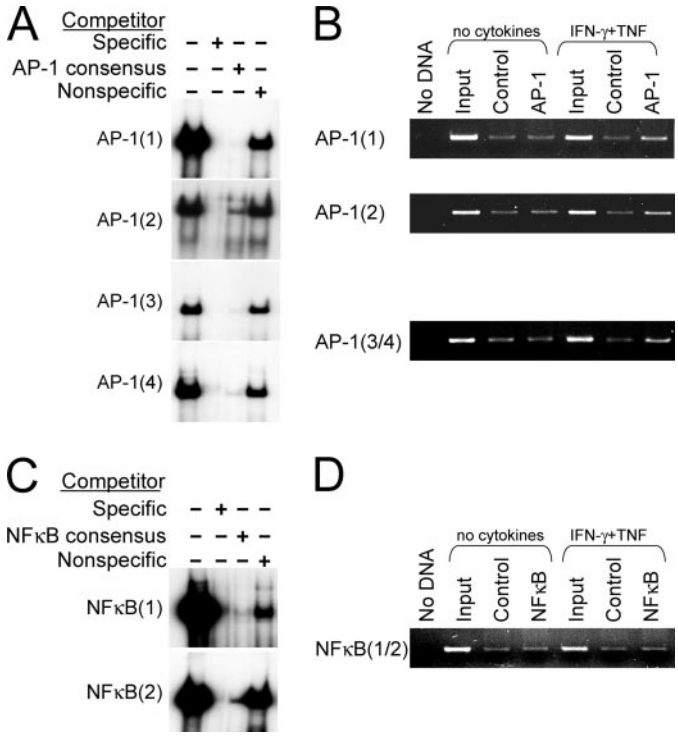

FIGURE 8. **EMSA and ChIP analyses indicate transcription factor binding to sites within the human long MLCK promoter.** *A,* EMSA was used to assess protein binding to potential transcription factor binding sites. All four of the AP-1 sites within the promoter show protein binding that can be specifically competed with cold site-specific or consensus AP-1 probes. Data shown are representative of three similar experiments. *B,* chromatin from IFN-γ-primed (18 h) and TNF-treated (3 h) Caco-2 monolayers was immunoprecipitated using antibodies against Jun protein. PCR detection of the AP-1 sites shows increased binding of AP-1 to the indicated regions of the promoter after 3 h TNF treatment. Data shown are representative of two similar experiments. *C,* EMSA analyses of potential NFκB sites within the promoter show protein binding that can be specifically competed with cold site-specific or consensus NFκB probes. Data shown are representative of three similar experiments. *D*, chromatin from IFN-γ-primed (18 h) and TNF-treated (3 h) Caco-2 monolayers was immunoprecipitated using antibodies against NFκB protein. PCR detection of the NFκB sites shows little specific binding of NFκB to the region of the promoter containing NFκB sites either before or after 3 h of TNF treatment. Data shown are representative of two similar experiments.

Similar site-directed mutagenesis of the NFκB (1) and NFκB (2) sites showed that mutation of either site completely blocked transcription by the p50–65 fusion protein (Fig. 9*B*). This suggests that both NFκB binding sites identified are required for MLCK transcriptional activation by NFκB.

TNF-induced MLCK Promoter Activation Only Occurs in Well Differentiated Intestinal Epithelial Monolayers—The transcription factors involved in TNF-induced MLCK up-regulation have been a subject of controversy, with conflicting results in separate studies using different Caco-2 cell clones grown under different conditions (10, 11). In comparing these studies one obvious difference is the differentiation state of the Caco-2 monolayers used. We used a well differentiated Caco-2_{BBE} subclone (19) grown for at least 2 weeks after confluence to allow for complete epithelial differentiation (10, 27–29). In contrast, others used the less well differentiated Caco-2 parental line (11). We therefore considered the possibility that differences in results obtained could be caused by differences in epithelial differentiation state.

To model the process of intestinal epithelial differentiation, we studied Caco-2_{BBE} monolayers 3 days after reaching confluence, as well as at early, 7 days, and late, 14 days, in the differentiation process. This is a well established model of intestinal epithelial differentiation that is thought to recapitulate the process that occurs *in vivo* as cells migrate from crypt to villus (8, 28–33). The data show that TNF did not significantly up-regulate transcription from the full-length 4-kb MLCK promoter in undifferentiated monolayers studied after 3 or 7 days (Fig. 10*A*). In contrast, at 14 days, when monolayers were well differentiated, the 4-kb MLCK promoter was fully responsive to TNF after priming with IFN-γ (Fig. 10*A*). This suggests that the signaling pathways activated by TNF must differ between undifferentiated and well differentiated intestinal epithelial cells.

To determine if activation of NFκB- or AP-1-mediated transcription by TNF was modulated during intestinal epithelial differentiation, monolayers transfected with the consensus NFκB or AP-1 reporter constructs were studied 3 days, 7 days, and 14 days after confluence. Remarkably, TNF-induced NFκB

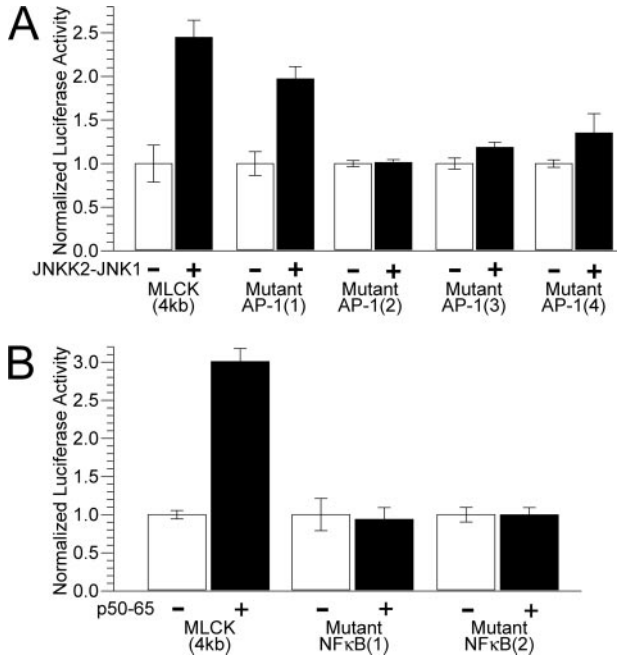

FIGURE 9. **Site-directed mutagenesis reveals the functional roles of transcription factor binding sites.** *A,* wild type and mutant promoter constructs were cotransfected with the JNKK2-JNK1 expression construct to test the role of each identified AP-1 binding site. The data show that activation of the 4-kb wild-type promoter requires AP-1 (2), AP-1 (3), and AP-1 (4) sites. The AP-1 (1) mutant only shows a small decrease in transcriptional activation relative to the wild type. Data shown are mean ± S.E. of triplicate samples, normalized to transfection with the promoter construct and an empty vector, and are representative of four similar experiments. *B,* wild type and mutant promoter constructs were cotransfected with the p50–65 expression construct to test the role of each identified NFκB binding site. The data show that activation of the 4-kb wild type promoter requires both NFκB sites. Data shown are mean ± S.E. of triplicate samples, normalized to transfection with the promoter construct and an empty vector, and are representative of four similar experiments.

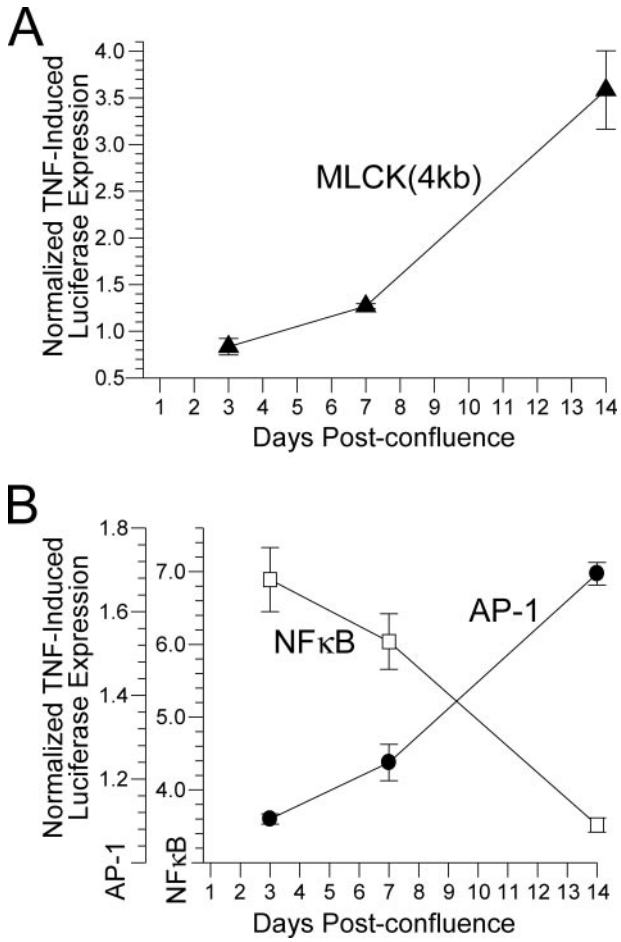

FIGURE 10. **Epithelial differentiation state modulates TNF-dependent MLCK promoter activation and transcription factor responses.** *A,* Caco-2 cells transfected with the 4-kb MLCK promoter construct were cultured on Transwells for the times indicated to allow varying extents of differentiation. At each time point, monolayers primed with IFN-γ for 18 h were treated with TNF for 8 h. The 4-kb long MLCK promoter was only activated by TNF in well differentiated monolayers. Data shown are mean ± S.E. of triplicate samples, normalized to identical IFN-γ-primed monolayers not treated with TNF, and are representative of three similar experiments. *B,* Caco-2 cells transfected with either the AP-1 reporter construct (*open circles*) or the NFκB reporter construct (*closed boxes*). Monolayers were allowed to differentiate, primed with IFN-γ, and treated with TNF for 8 h as above. AP-1 signaling in response to TNF increased during differentiation, while NFκB signaling diminished. These results indicate that differentiation status modifies the signaling response to TNF. Data shown are mean ± S.E. of triplicate samples, normalized to identical IFN-γ-primed monolayers not treated with TNF, and are representative of three similar experiments.

activation diminished during the process of epithelial differentiation (Fig. 10*B*). Conversely, TNF-induced AP-1 activation increased during epithelial differentiation (Fig. 10*B*). These data suggest that signaling pathways activated by TNF are modulated by epithelial differentiation. Moreover, the data may explain differences in the reported roles of specific transcription factor pathways in MLCK up-regulation reported by various laboratories (10, 11).

DISCUSSION

MLCK-dependent actomyosin regulation is central to control of many essential cellular processes, including contraction, migration, and epithelial barrier function (27, 34–39). In many nonmuscle cells, long and short MLCK are co-expressed from two different promoters within a single gene (2, 3). When both MLCK proteins are expressed in a single cell, short MLCK tends to associate with myosin IIA, but not F-actin, while long MLCK associates with dense F-actin bundles, but not myosin IIA (4). This suggests that, even when expressed in a single cell, long and short MLCK proteins serve unique functions.

Some cell types primarily express only long or short MLCK. For example, we have recently shown that long MLCK is the principal MLCK expressed in intestinal epithelial cells (8). Moreover, we have shown that long MLCK is associated with the perijunctional ring of actomyosin and that the activity of long MLCK can regulate tight junction permeability, *i.e.* epithelial barrier function (8, 27). Similar roles for MLCK have been reported in other epithelial tissues and vascular endothelia (40–42). We have recently shown that MLCK activation is necessary for the loss of barrier function induced by TNF, both *in vitro* and *in vivo* (12, 16). This increased MLCK activity is associated with increased MLCK expression (10, 11), and similar increases in MLCK expression and activity are present in intestinal epithelia of inflammatory bowel disease patients (17). Thus, it is likely that inducible long MLCK expression plays an important role in disease pathogenesis. It is, however, impossible to assess the potential therapeutic efficacy of pharmacological agents that modify gene transcription without detailed

understanding of the mechanisms that regulate long MLCK expression.

Our data represent the first comprehensive analysis of the elements necessary for human long MLCK transcription. Thus, while we used cultured human intestinal epithelial cells as our model system, the data are likely to have significant implications in many other cell types. Additionally, our data provide new insights into the structure of the long MLCK, or MYLK, gene. We performed the first 5′-RACE analysis to identify the 5′-untranslated region of long MLCK. In doing so we discovered two previously unrecognized exons that are alternatively used as the transcriptional start site. This observation has important implications, as 31 kb of intronic sequence upstream of exon 1B may represent a unique promoter for that transcriptional start site.

Because of the location of potential binding sites for AP-1 and NFκB, we focused our attention on transcription from exon 1A. We therefore cloned the 4-kb region and used a standard reporter assay to identify the minimal sequence necessary for long MLCK transcription. The data show that this information is contained within the first 278 bp 5′ to the transcriptional start site and includes 2 Sp1 sites but no TATA box. These analyses also suggest that transcriptional repressors are located within the region from −1588 to −618 relative to the long MLCK transcriptional start site. We then determined that the full-length 4-kb sequence was able to respond to TNF in a manner similar to the endogenous promoter.

To identify the mechanism by which the 4-kb sequence activated transcription in response to TNF we first asked whether the long MLCK promoter was responsive to NFκB or AP-1 activation. These transcription factor signaling pathways are both activated by TNF and, in the case of TNF-dependent intestinal epithelial long MLCK protein up-regulation, the role of NFκB has been the subject of controversy (10, 11). Our previous work has shown that TNF-dependent intestinal epithelial long MLCK protein up-regulation does not require NFκB activation (10). This is consistent with the absence of *in vivo* NFκB binding to MLCK promoter sequences, as determined by ChIP analyses. Although Ma *et al.* (11) also reported that TNF could induce increases in Caco-2 MLCK expression, they found that this up-regulation was blocked by NFκB inhibition. Ma *et al.* recently reported that the a single NFκB binding site mediates a 50% increase in transcription in response to TNF (43). We have located this site ~150bp upstream of exon 1A, downstream of the 3′ Sp1 site. While this NFκB site was scored as a low probability NFκB binding site by the algorithm we used for our initial *in silico* analysis, we have noted that the region including this site does augment transcription induced by p50–65 by 0.2 ± 0.05-fold relative to a deletion construct lacking this region ($p = 0.01$).[4] Thus, whereas our data are consistent with a minor role for this site, it is unlikely to be the major upstream element critically involved in long MLCK transcriptional regulation from exon 1A.

We used a combination of EMSA, ChIP, and site-directed mutagenesis approaches to identify 2 NFκB and 3 AP-1 sites that were required for NFκB- and AP-1-mediated long MLCK transcriptional activation, respectively. We found that transcription from the long MLCK promoter could be activated by NFκB but was also activated by AP-1. However, TNF was only able to activate transcription from the long MLCK promoter in well differentiated intestinal epithelial monolayers. We also found that an NFκB consensus promoter reporter was better activated by TNF in undifferentiated monolayers, while an AP-1 consensus promoter reporter was better activated by TNF in well differentiated monolayers. This result provides a potential explanation for divergent results, as it may be that NFκB mediates long MLCK transcriptional activation in undifferentiated cells while AP-1 is more important in differentiated cells. That is, the differentiation state of the intestinal epithelial monolayers studied may modulate the response to TNF in terms of the transcription factor pathways activated.

These data prompt one to ask why the intestinal epithelium would use two different transcription factor pathways to increase long MLCK expression. What is so different about the undifferentiated and well differentiated Caco-2 monolayers? To understand this, it is important to recognize that undifferentiated monolayers are most like intestinal crypt epithelium while well differentiated monolayers model villus epithelium (28–33). Undifferentiated crypt epithelium is specialized for proliferation and ion secretion. Thus, one might hypothesize that NFκB activation in response to TNF would be important, as NFκB can activate anti-apoptotic cytoprotective events, in part through down-regulating JNK activation (26), and crypt cell survival is critical to intestinal homeostasis. In contrast, TNF-induced JNK activation can promote apoptosis (26). Such apoptosis may in fact be a physiologically appropriate response in the face of intestinal injury. For example, in mice with an intestinal epithelial cell-specific knock-out leading to an inability to activate NFκB, intestinal ischemia-reperfusion injury results in increased villus cell loss compared with wild-type mice (44). Paradoxically, this is beneficial, as the knock-out animals with increased enterocyte damage are protected from the multi-organ failure that follows intestinal ischemia-reperfusion injury (44). Alternatively, the observations that the intestine-specific Cdx-2 homeobox gene is necessary for villus cell differentiation (45, 46) and that TNF down-regulates Cdx-2 via an NFκB-dependent pathway (47) might explain the reduced TNF-dependent NFκB activation in well differentiated villus-like cell. Whatever the explanation, the data do show that intestinal epithelial transcription factor responses to TNF are modulated by cell differentiation state.

In summary, our data identify two unique 5′-untranslated regions corresponding to two novel alternatively utilized exons and transcriptional start sites for human long MLCK. We are also the first to comprehensively characterize the mammalian promoter for long MLCK transcribed from exon 1A. This is of biological and, potentially, therapeutic importance, given the critical and diverse roles of long MLCK in disease. Moreover, the data suggest that the differentiation state of intestinal epithelial, and perhaps other, cells can profoundly influence cytokine-induced transcriptional activation.

[4] W. V. Graham and J. R. Turner, unpublished observations.

Acknowledgments—We thank Amanda Marchiando, Le Shen, and Judy Turner for their insightful comments at various stages of these studies.

REFERENCES

1. Kamm, K. E., and Stull, J. T. (2001) *J. Biol. Chem.* **276,** 4527–4530
2. Garcia, J. G., Lazar, V., Gilbert-McClain, L. I., Gallagher, P. J., and Verin, A. D. (1997) *Am. J. Respir. Cell Mol. Biol.* **16,** 489–494
3. Yin, F., Hoggatt, A. M., Zhou, J., and Herring, B. P. (2006) *Am. J. Physiol.* **290,** C1599–C1609
4. Blue, E. K., Goeckeler, Z. M., Jin, Y., Hou, L., Dixon, S. A., Herring, B. P., Wysolmerski, R. B., and Gallagher, P. J. (2002) *Am. J. Physiol. Cell Physiol.* **282,** C451–C460
5. Gallagher, P. J., and Herring, B. P. (1991) *J. Biol. Chem.* **266,** 23945–23952
6. Herring, B. P., and Smith, A. F. (1996) *Am. J. Physiol.* **270,** C1656–C1665
7. Gallagher, P. J., Garcia, J. G., and Herring, B. P. (1995) *J. Biol. Chem.* **270,** 29090–29095
8. Clayburgh, D. R., Rosen, S., Witkowski, E. D., Wang, F., Blair, S., Dudek, S., Garcia, J. G., Alverdy, J. C., and Turner, J. R. (2004) *J. Biol. Chem.* **279,** 55506–55513
9. Kudryashov, D. S., Chibalina, M. V., Birukov, K. G., Lukas, T. J., Sellers, J. R., Van Eldik, L. J., Watterson, D. M., and Shirinsky, V. P. (1999) *FEBS Lett.* **463,** 67–71
10. Wang, F., Graham, W. V., Wang, Y., Witkowski, E. D., Schwarz, B. T., and Turner, J. R. (2005) *Am. J. Pathol.* **166,** 409–419
11. Ma, T. Y., Boivin, M. A., Ye, D., Pedram, A., and Said, H. M. (2005) *Am. J. Physiol. Gastrointest. Liver Physiol.* **288,** G422–G430
12. Zolotarevsky, Y., Hecht, G., Koutsouris, A., Gonzalez, D. E., Quan, C., Tom, J., Mrsny, R. J., and Turner, J. R. (2002) *Gastroenterology* **123,** 163–172
13. Hecht, G., Pestic, L., Nikcevic, G., Koutsouris, A., Tripuraneni, J., Lorimer, D. D., Nowak, G., Guerriero, V., Jr., Elson, E. L., and Lanerolle, P. D. (1996) *Am. J. Physiol.* **271,** C1678–C1684
14. Shen, L., Black, E. D., Witkowski, E. D., Lencer, W. I., Guerriero, V., Schneeberger, E. E., and Turner, J. R. (2006) *J. Cell Sci.* **119,** 2095–2106
15. Clayburgh, D. R., Shen, L., and Turner, J. R. (2004) *Lab. Investig.* **84,** 282–291
16. Clayburgh, D. R., Barrett, T. A., Tang, Y., Meddings, J. B., Van Eldik, L. J., Watterson, D. M., Clarke, L. L., Mrsny, R. J., and Turner, J. R. (2005) *J. Clin. Investig.* **115,** 2702–2715
17. Blair, S. A., Kane, S. V., Clayburgh, D. R., and Turner, J. R. (2006) *Lab. Investig.* **86,** 191–201
18. Suenaert, P., Bulteel, V., Lemmens, L., Noman, M., Geypens, B., Van Assche, G., Geboes, K., Ceuppens, J. L., and Rutgeerts, P. (2002) *Am. J. Gastroenterol.* **97,** 2000–2004
19. Peterson, M. D., and Mooseker, M. S. (1992) *J. Cell Sci.* **102,** 581–600
20. Turner, J. R., Lencer, W. I., Carlson, S., and Madara, J. L. (1996) *J. Biol. Chem.* **271,** 7738–7744
21. Heinemeyer, T., Wingender, E., Reuter, I., Hermjakob, H., Kel, A. E., Kel, O. V., Ignatieva, E. V., Ananko, E. A., Podkolodnaya, O. A., Kolpakov, F. A., Podkolodny, N. L., and Kolchanov, N. A. (1998) *Nucleic Acids Res.* **26,** 362–367
22. Lazar, V., and Garcia, J. G. (1999) *Genomics* **57,** 256–267
23. Zheng, C., Xiang, J., Hunter, T., and Lin, A. (1999) *J. Biol. Chem.* **274,** 28966–28971
24. Kunsch, C., Ruben, S. M., and Rosen, C. A. (1992) *Mol. Cell. Biol.* **12,** 4412–4421
25. Varfolomeev, E. E., and Ashkenazi, A. (2004) *Cell* **116,** 491–497
26. De Smaele, E., Zazzeroni, F., Papa, S., Nguyen, D. U., Jin, R., Jones, J., Cong, R., and Franzoso, G. (2001) *Nature* **414,** 308–313
27. Turner, J. R., Rill, B. K., Carlson, S. L., Carnes, D., Kerner, R., Mrsny, R. J., and Madara, J. L. (1997) *Am. J. Physiol.* **273,** C1378–C1385
28. Pinto, M., Robine-Leon, S., Appay, M. D., Kedinger, M., Triadou, N., Dussaulx, E., Lacroix, B., Simon-Assmann, P., Haffen, K., Fogh, J., and Zweibaum, A. (1983) *Biol. Cell* **47,** 323–330
29. Van Beers, E. H., Al, R. H., Rings, E. H., Einerhand, A. W., Dekker, J., and Buller, H. A. (1995) *Biochem. J.* **308,** 769–775
30. Shorter, R. G., Moertel, C. G., Titus, J. L., and Reitemeier, R. J. (1964) *Am. J. Dig. Dis.* **13,** 760–763
31. Peterson, M. D., Bement, W. M., and Mooseker, M. S. (1993) *J. Cell Sci.* **105,** 461–472
32. Chandrasena, G., Sunitha, I., Lau, C., Nanthakumar, N. N., and Henning, S. J. (1992) *Cell Mol. Biol.* **38,** 243–254
33. Fleet, J. C., Wang, L., Vitek, O., Craig, B. A., and Edenberg, H. J. (2003) *Physiol. Genomics* **13,** 57–68
34. Peterson, L. J., Rajfur, Z., Maddox, A. S., Freel, C. D., Chen, Y., Edlund, M., Otey, C., and Burridge, K. (2004) *Mol. Biol. Cell* **15,** 3497–3508
35. Kamm, K. E., and Stull, J. T. (1986) *Science* **232,** 80–82
36. Itoh, T., Ikebe, M., Kargacin, G. J., Hartshorne, D. J., Kemp, B. E., and Fay, F. S. (1989) *Nature* **338,** 164–167
37. Russo, J. M., Florian, P., Shen, L., Graham, W. V., Tretiakova, M. S., Gitter, A. H., Mrsny, R. J., and Turner, J. R. (2005) *Gastroenterology* **128,** 987–1001
38. Giannone, G., Dubin-Thaler, B. J., Dobereiner, H.-G., Kieffer, N., Bresnick, A. R., and Sheetz, M. P. (2004) *Cell* **116,** 431–443
39. Berglund, J. J., Riegler, M., Zolotarevsky, Y., Wenzl, E., and Turner, J. R. (2001) *Am. J. Physiol. Gastrointest Liver Physiol.* **281,** G1487–G1493
40. Yamaguchi, Y., Dalle-Molle, E., and Hardison, W. G. (1991) *Am. J. Physiol.* **261,** G312–G319
41. Goeckeler, Z. M., and Wysolmerski, R. B. (1995) *J. Cell Biol.* **130,** 613–627
42. Garcia, J. G., Davis, H. W., and Patterson, C. E. (1995) *J. Cell. Physiol.* **163,** 510–522
43. Ye, D., Ma, I., and Ma, T. Y. (2006) *Am. J. Physiol. Gastrointest Liver Physiol.* **290,** G496–G504
44. Chen, L. W., Egan, L., Li, Z. W., Greten, F. R., Kagnoff, M. F., and Karin, M. (2003) *Nat. Med.* **9,** 575–581
45. Silberg, D. G., Swain, G. P., Suh, E. R., and Traber, P. G. (2000) *Gastroenterology* **119,** 961–971
46. Lorentz, O., Duluc, I., Arcangelis, A. D., Simon-Assmann, P., Kedinger, M., and Freund, J. N. (1997) *J. Cell Biol.* **139,** 1553–1565
47. Kim, S., Domon-Dell, C., Wang, Q., Chung, D. H., Di Cristofano, A., Pandolfi, P. P., Freund, J.-N., and Evers, B. M. (2002) *Gastroenterology* **123,** 1163–1178